Presented at the DLSU Research Congress 2015
De La Salle University, Manila, Philippines
March 2-4, 2015

Green Luminescence from Spatially Distributed Zinc Sulfide (ZnS) Nanostructures Prepared via Horizontal Vapor Phase Crystal Growth (HVPCG)

Kiveen P. Suycano[1,2*], Gil Nonato C. Santos[1], Reuben V. Quiroga[1]
[1] *De La Salle University, Manila*
[2] *Industrial Technology Development Institute, DOST*
[*] *kivsrose@gmail.com*

Abstract: Zinc Sulfide (ZnS) Nanostructures consisting nanorods, nanosheets, nanoribbons, nanostrips, and nanowindmills were successfully synthesized from ~35 mg ZnS powder via Horizontal Vapor Phase Crystal Growth (HVPCG) at 1000 ^{0}C growth temperature, 4 hours dwell time, and 80 minutes ramp time. The synthesized nanomaterials were characterized using Scanning Electron Microscopy (SEM), Energy Dispersive X-ray (EDX) analyses, Photoluminescence (PL) Spectroscopy, and X-ray Diffraction (XRD). The nanomaterials were deposited at the cold zone only in either simultaneous or sequential manner. SEM images were taken consecutively in a row from cold zone end to hot zone end of the deposit. It was observed that nanorods, nanosheets, nanoribbons, nanostrips, and nanowindmills were respectively deposited in order. EDX compositional analyses revealed that the atomic composition of the as-grown ZnS nanostructures have deficiency in sulfur. This is also supported by the PL investigation in which the deposit exhibited green at ~530 nm luminescence. X-ray diffraction test result attests that the deposited nanomaterials have wurtzite crystal structure.

Keywords: Zinc Sulfide; Nanostructures; Luminescence; Wurtzite

1. INTRODUCTION

Much attention has been given to Zinc Sulfide (ZnS) because of its unique properties. As early as the advent of the 21st century, researchers began to synthesize and characterize ZnS nanomaterials for possible applications in the electronics industry.

ZnS is a photoluminescent material. It is advantageously doped with elements such as Tb, Eu, Mn, Pb, Au, Ag, Fe, Cu, etc. due to its wide bandgap of 3.7 eV at 300K so that it can produce a wide range of exciting optical properties (Son et al., 2007). This semiconductor material has a high refractive index and a high transmittance in the visible range. In terms of crystal structure, ZnS has two types: hexagonal wurtzite phase and cubic zinc blende phase depending on synthesis conditions. Typically, the stable structure at room temperature is the zinc blende, with few observances of stable wurtzite ZnS [2].

In this study, wurtzite ZnS powder was used as the source material. The structure of wurtzite ZnS can be described as tetrahedrally synchronized S^{2-} and Zn^{2+} ions, arranged alternately along the c-axis as shown in fig. 1, results in non-central symmetric structure and piezoelectricity. Another significant characteristic of wurtzite ZnS is the polar surfaces. The positively charged Zn-(0001) and negatively charged S-$(000\bar{1})$ polar surfaces

produces a normal dipole moment. Spontaneous polarization occurs along c-axis as well as divergence in surface energy. The three fastest growth directions of ZnS are $<2\bar{1}\bar{1}0>(\pm[2\bar{1}\bar{1}0],\pm[\bar{1}2\bar{1}0],\pm[\bar{1}\bar{1}20])$; $<01\bar{1}0>(\pm[01\bar{1}0],\pm[10\bar{1}0],\pm[1\bar{1}00])$; and $\pm[0001]$. By adjusting these growth directions, different morphologies can be observed (Ma et al., 2003).

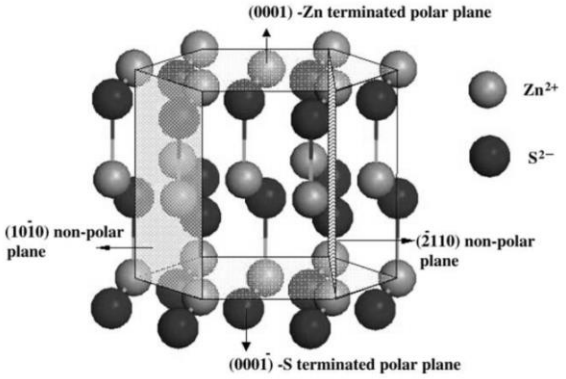

Figure 1. Structure model of wurtzite ZnS (Moore et al., 2004)

Various techniques have been developed in the growth and preparation of nanostructured materials. Wilson and co-authors mapped six widely known methods to produce nanomaterials. These are plasma arcing, chemical vapour deposition, electrodeposition, sol-gel synthesis, ball milling, and the use of natural nanoparticles (Wilson et al., 2002). Moreover, Cao imposed four technique categories namely, (1) spontaneous growth which includes evaporation-condensation, vapor-liquid-solid growth and stress-induced recrystallization (2) template-based synthesis which includes electroplating and electrophoretic deposition, colloid dispersion, melt or solution filling, and conversion with chemical reaction (3) electrospinning (4) lithography (Cao, 2004).

Chander reviewed strategies in the synthesis of nanophosphors. It is observed that the field of nano luminescent materials is immensely resonant and dynamic. Diverse processes have been developed such as chemical precipitation with and without capping agents, sol-gel, sol-gel with heating, microemulsion, solid state heating, chemical vapour synthesis, hydrothermal synthesis, chemical synthesis within matrix, molecular beam epitaxy, electrochemical route, autocombustion, and chemical precipitation from homogeneous solution. However, despite the said achievements, some are still not likely to be technologically acceptable since they are not economically and environmentally friendly which includes the processes of sol-gel, sol-gel with heating, microemulsion, chemical vapour synthesis, molecular beam epitaxy and autocombustion (Chander, 2006).

The nanostructures investigated in this paper were synthesized via horizontal vapor phase crystal growth (HVPCG) by way of a thermal evaporation technique without any carrier gas. In principle, the HVPCG is a simple technique in which the source material is vaporized at elevated temperatures and then the resulting vapor condenses and solidifies again under certain conditions (temperature, pressure, atmosphere, substrate, etc.) to form nanomaterials.

2. METHODOLOGY

Approximately 35 mg of ZnS with 99.9% purity was sealed inside a clean oven toaster tube attached to a Thermionics high vacuum system using oxy-acetelane. The tube was depressurized to a magnitude of ~10^{-6} torr to remove any gas impurities that may affect the growth of nanomaterials. The sealed tube was then loaded into a Thermolyne horizontal tube furnace (Fig. 2) programmed at 1000 ^{0}C growth temperature, 4 hours dwell time, and 80 min ramp time. The tube was sectioned into two regions; the **hot zone**, which is inside the furnace and the **cold zone**, which is outside.

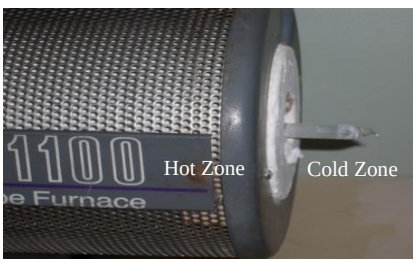

Figure 2. Tube loaded partially into the furnace

The synthesized nanomaterials were characterized using Scanning Electron Microscopy (SEM), Energy Dispersive X-ray (EDX) analyses, Photoluminescence Spectrometry (PL), and X-ray Diffraction (XRD).

3. RESULTS AND DISCUSSIONS

The formation of these novel ZnS nanostructures can be explained in terms of vapor-solid (V-S) growth mechanism. When the energy is enough to sublime the powder, the sublimated vapor begins to move until it reaches the energetically favorable region where deposition occurs. The movement is possible because of the temperature difference between hot zone (~1000 ^{0}C) and cold zone (~350 ^{0}C).

As the source material vaporizes from the hot zone, the sublimated vapor is then deposited at the cold zone which is of lower temperature (Fig. 3). At this time ZnS nanostructures starts to grow by self-catalyzing process since HVPCG is a catalyst-free method.

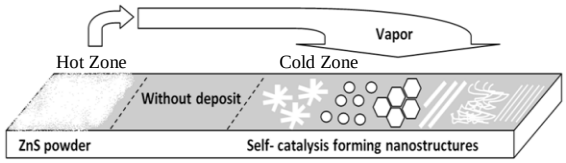

Figure 3. Schematic of deposition process by HPVCG

3.1 Novel ZnS Nanostructures

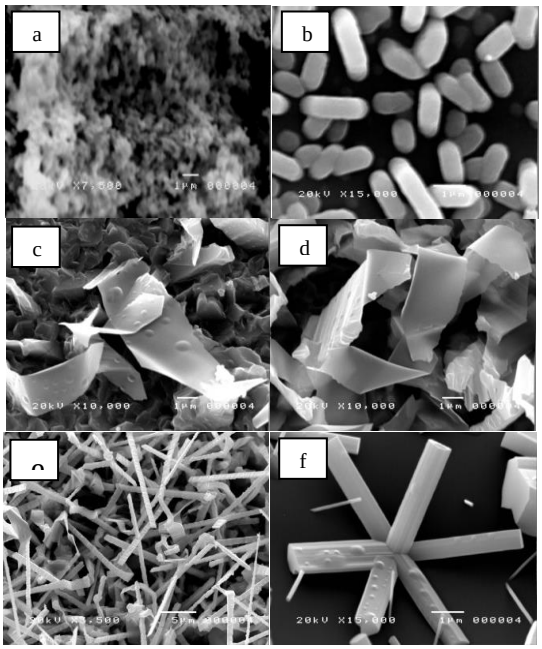

Figure 4. JEOL JSM-5310 SEM images of ZnS
(a) powder (b) nanorods (c) nanosheets (d) nanoribbons (e) nanostrips and (f) nanowindmills.

Five kinds of ZnS nanostructures have been found using the scanning electron microscope (SEM). The images were taken consecutively in a row from cold zone to hot zone. It was observed that nanorods, nanosheets, nanoribbons, nanostrips, and nanowindmills were respectively deposited in order.

Measurements of the dimensions of the nanostructures were done using the SemAfore software which is provided by JEOL.

3.2 Energy Dispersive X-ray (EDX) Analysis

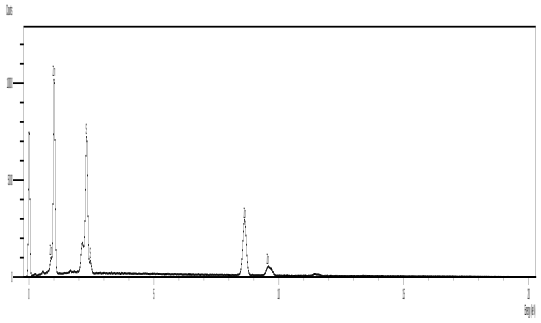

Figure 5. EDX spectrum of the deposited ZnS nanomaterials

The above figure displays the representative EDX spectrum of the deposited ZnS nanomaterials on the wall of the tube used in the synthesis. The atomic percentage values are presented in table 1.

Table 1. The nanostructures respective size and atomic composition.

No.	Structure	Size (nm)	Atomic Composition (%)	
			Zn	S
1	nanorods	~600	69.22	30.78
2	nanosheets	~30	64.01	35.99
3	nanoribbons	~50	66.70	33.30
4	nanostrips	~255	61.50	38.50
5	nanowindmills	~550-900	69.49	30.51

In table 1, the type of structure is listed according to its occurrence with respect to the cold zone. The standard deviation of the Zn and S atomic composition values (~2.8) implies that the values are statistically close to each other. Hence, the values for Zn and S are not a function of the distance from the hot zone to the cold zone.

3.3 Photoluminescence Study

Photoluminescence investigation was carried out using a UV lamp with peak centered at ~355 nm as the excitation source. Relative to the bandgap of the source ZnS powder which is 3.7eV at 300K, the excitation wavelength was calculated to be around 335nm.

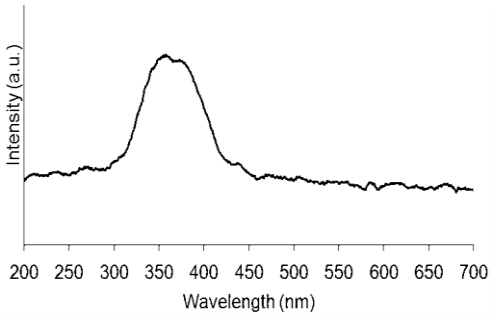

Figure 6. Spectrum of the excitation source (UV Lamp)

Room temperature photoluminescence property of the ZnS deposit was investigated using Ocean Optics Spectrometer. However, it was not possible to determine which structure(s) exhibited green luminescence because they co-existed with the background microstructures and thin film.

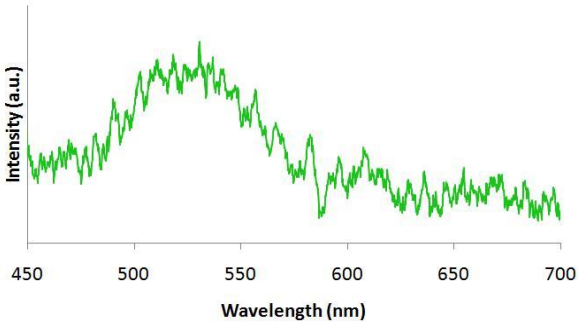

Fig. 7. Photoluminescence (PL) spectrum of ZnS nanostructures

Figure 7 shows green luminescence with PL peak centered at around 530nm. The PL peak obtained in the study found similar results previously conveyed in the scientific community. A PL peak at ~530nm for ZnS nanorods was identified by Senthilkumaar and Thamiz Selvi using a 280nm source (Senthilkumaar et al., 2008). Two PL peaks at ~483nm and ~561nm were observed by Sharma and co-workers upon exposing their PVP capped ZnS nanoparticles to a 280nm source (Sharma et al., 2008) while Shen and co-researchers got a PL peak for ZnS nanowires arrays at ~554nm using He-Cd laser with 325nm wavelength (Shen et al., 2008). Wu

and co-members obtained a PL peak for ZnS nanoparticles at ~480nm with a 420nm-Xe lamp as the excitation source (Wu et al, 2006).

The result of the PL analysis in this study is an indication of stoichiometric defects (Senthilkumaar et al., 2008), which might be a vacancy or an interstitial state (Callister, 2007). The composition analysis by EDX supports the existence of sulfur deficiency (Gosh et al., 2006) of the deposited ZnS nanomaterials. Using the equation $E=hc/\lambda$, the calculated photoluminescence energy is 2.34 eV.

3.4 X-ray Diffraction (XRD) Investigations

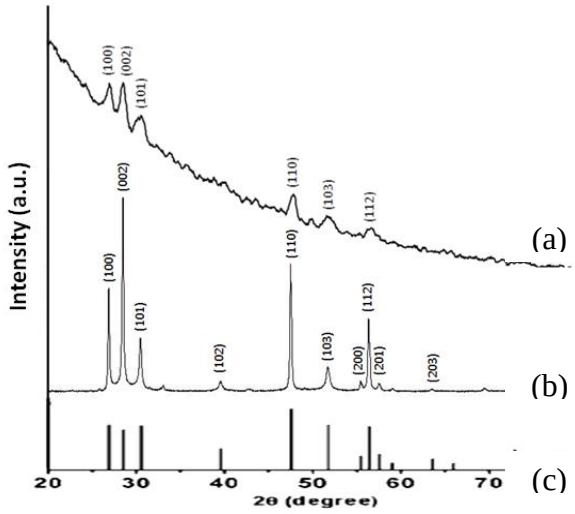

Fig. 8. XRD spectra of wurtzite ZnS (a) deposit (b) source powder (c) JCPDS PDF card no. 36-1450

Figure 8 shows the XRD patterns of the deposit, the source powder, and the standard diffraction peaks of wurtzite ZnS. All the intense peaks of the XRD spectrum of the deposit can be indexed to a wurtzite ZnS structure with a (002) dominant peak denoting a high single-crystalline material.

4. CONCLUSIONS

High single-crystalline ZnS nanorods, nanosheets, nanoribbons, nanostrips, and nanowindmills have been successfully grown via horizontal vapor phase crystal growth (HVPCG) at 1000 ^{0}C, and dwelt for 4 hours. The deposit exhibited green luminescence centered at around 530 nm. The calculated photoluminescence energy is 2.34 eV. The consolidated results of the morphology and composition analyses, photoluminescence studies, and x-ray diffraction investigations brings the authors to a conclusion that the as-synthesized nanomaterials namely the nanorods, nanosheets, nanoribbons, nanostrips, and nanowindmills are good candidates as nanophospors which may find possible applications in the optoelectronic industry.

5. ACKNOWLEDGMENT

KPS[1] thanks DOST-SEI for the Scholarship Grant and funding of this study.

6. REFERENCES

Callister Jr., W. D. (2007). Materials Science and Engineering: An Introduction, 7th ed., New York, USA: John Wiley & Sons, Inc.

Cao, G. (2004). Nanostructures and Nanomaterials: Synthesis, Properties and Applications, Covent Garden, London: Imperial College Press.

Chander, H. (2006) A Review on Synthesis of Nanophosphors – Future Luminescent Materials. Proc. of ASID '06, 11-15.

Gosh, P.K., Jana, S., Nandy, S., & Chattopadhyay, K.K. (2006). Size-dependent optical and dielectric properties of nanocrystalline ZnS thin films synthesized via rf-magnetron sputtering technique. Materials Research Bulletin, 42, 505-514.

Ma, C., Moore, D., Ding, Y., Li, J. & Wang, Z. (2004). Nanobelt and nanosaw structures of II-IV Semiconductors. Int. J. Nanotechnology, 1, 431-451.

Ma, C., Moore, D., Li, J. & Wang, Z. (2003). Nanobelts, Nanocombs, and Nanowidmills of Wurtzite ZnS. Advance Materials, 15, 228-231.

Moore, D., Ronning, C., Ma, C., & Wang, Z. (2004). Wurtzite ZnS nanosaws produced by polar surfaces. Chemical Physics Letters, 385, 8-11.

Peng, W.Q., Cong, G.W., Qu, S.C., & Wang, Z.G. (2006). Synthesis and photoluminescence of ZnS:Cu nanoparticles. Optical Materials, 29, 313-317.

Senthilkumaar, S. & Thamiz Selvi, R. (2008). Formation and Photoluminescence of Zinc Sulfide Nanorods. Journal of Applied Sciences, 8, 2306-2311.

Sharma, M., Kumara, S., & Pandey, O.P. (2008). Photo-physical and Morphological studies of Organically Passivated Core-Shell ZnS Nanoparticles. Digest Journal of Nanomaterials and Biostructures, 3, 189-197.

Shen, G., Bando, Y., Golberg, D. & Zhou, C. (2008). Heteroepitaxial Growth of Orientation-Ordered ZnS Nanowire Arrays. J. Phys. Chem., 30.

Son, D., Jung, D-R., Kim, J., Moon, T., C. Kim, & Park, B. (2007). Synthesis and photoluminescence of Mn-doped zinc sulphide nanoparticles. Applied Physics Letter, 90, 101910- 1 - 101910-3.

Wei, F., Li, G., & Zhang, Z. (2005). Hydrothermal synthesis of spindle-like ZnS hollow nanostructures. Materials Research Bulletin, 40, 1402-1407.

Wilson, M., Kannangara, K., Smith, G., Simmons, M., & Raguse,B. (2002). Nanotechnology: Basic Science and Emerging Technologies, Australia. CRC Press.

Wu,Y., Hao, X., Yang, J., Tian, F., & Jiang, M. (2006). Ultrasound-assisted synthesis of nanocrystalline ZnS in the ionic liquid [BMIM].BF4. Materials Letters, 60, 2764-2766.